ISSN (Print) 1226-1750
ISSN (Online) 2233-6656
Journal of Magnetics 19(2), 185-191 (2014) http://dx.doi.org/10.4283/JMAG.2014.19.2.185

Analysis of Images According to the Fluid Velocity in Time-of-Flight Magnetic Resonance Angiography, and Contrast Enhancement Angiography

Eng-Chan Kim[1], Yeong-Cheol Heo[2,3], Jae-Hwan Cho[3], Hyun-Jeong Lee[1], and Hae-Kag Lee[4]*

[1]*Department of Physics, Yeungnam University, Gyeongsan 705-717, Korea*
[2]*Department of Radiology, Kyung Hee University Hospital at Gang-dong, Seoul 135-841, Korea*
[3]*Department of International Radiological Science, Hallym University of Graduate Studies, Seoul 135-841, Korea*
[4]*Department of Computer Science and Engineering, Soonchunhyang University, Asan 336-745 Korea*

(Received 12 April 2014, Received in final form 13 May 2014, Accepted 13 May 2014)

In this study we evaluated that flow rate changes affect the (time of flight) TOF image and contrast-enhanced (CE) in a three-dimensional TOF angiography. We used a 3.0T MR System, a nonpulsatile flow rate model. Saline was used as a fluid injected at a flow rate of 11.4 cm/sec by auto injector. The fluid signal strength, phantom body signal strength and background signal strength were measured at 1, 5, 10, 15, 20 and 25-th cross-section in the experienced images and then they were used to determine signal-to-noise ratio and contrast-to-noise ratio. The inlet, middle and outlet length were measured using coronal images obtained through the maximum intensity projection method. As a result, the length of inner cavity was 2.66 mm with no difference among the inlet, middle and outlet length. We also could know that the magnification rate is 49-55.6% in inlet part, 49-59% in middle part and 49-59% in outlet part, and so the image is generally larger than in the actual measurement. Signal-to-noise ratio and contrast-to-noise ratio were negatively correlated with the fluid velocity and so we could see that signal-to-noise ratio and contrast-to-noise ratio are reduced by faster fluid velocity. Signal-to-noise ratio was 42.2-52.5 in 5-25th section and contrast-to-noise ratio was from 34.0-46.1 also not different, but there was a difference in the 1st section. The smallest 3D TOF MRA measure was 2.51 ± 0.12 mm with a flow velocity of 40 cm/s. Consequently, 3D TOF MRA tests show that the faster fluid velocity decreases the signal-to-noise ratio and contrast-to-noise ratio, and basically it can be determined that 3D TOF MRA and 3D CE MRA are displayed larger than in the actual measurement.

Keywords : TOF angiography, fluid velocity, length of inner cavity, signal-to-noise ratio, contrast-to-noise ratio

1. Introduction

Cerebrovascular disease is a largely classified hemorrhagic and ischemic cerebrovascular disease. In the past of our country, the proportion of hemorrhagic cerebrovascular diseases was significantly higher than in the Western countries. However, the incidence of ischemic cerebrovascular diseases is increasing in recent years, and so the rate of ischemic cerebrovascular diseases is higher than of hemorrhagic cerebrovascular diseases like in the Western countries [1-4]. In the past, computed tomography (CT) and cerebral angiography have been primarily used to diagnose cerebrovascular diseases. Cerebral angiography in particular was recognized as an important and basic technique to confirm vascular obstruction ranging and the re-opening. In addition, CT images are acquired with very thin slices of the image at high speed, so they can implement the three-dimensional blood vessel images in various directions. At the same time, functional images like cerebral blood flow map images are performed also, so the importance of CT is emphasized to diagnose cerebrovascular diseases [5]. However, there are disadvantages such as the radiation burden and confusions caused by intravenous contrast as well as a brain fundus that may be covered by bone [6]. Recently, magnetic resonance imaging (MRI) is spread as diagnostic tool of brain diseases and comes into the spotlight. MRI is better than any other examinations regarding soft tissue contrast, and so it has been established as the primary diagnostic tool for brain-nervous system diseases.

With the advantage that cross-sectional images are possible without radiation and an assessment of the metabolites and functional images is provided as well as anatomical images MRI can be said the most advanced diagnostic imaging tests. In early years, the vascular obstruction diagnostic rate

*Corresponding author: Tel: +82-41-530-1276
Fax: +82-41-530-1548, e-mail: lhk7083@hanmail.net

was not high in, but the recently increasing fast-resolution recording technology shows more than 85% sensitivity and a specificity nearly 100% [7-10]. Digital subtraction angiography is generally considered as an important and essential test to evaluate a cerebrovascular angiostenosis because of its superior resolution and accuracy and it is still being used as an essential test of in most hospitals. However, magnetic resonance angiography (MRA) is increasingly used as a screening test because it is invasive and difficult to enforce in outpatient clinic.

MRA techniques are largely divided into phase technique using the phase of the signal, strength technique using the signal strength and contrast enhanced magnetic resonance angiography using contrast medium [11, 12]. In particular, TOF technique has been used as a screening assay because it is possible to test in short time without contrast medium [13]. However, the TOF technique has disadvantages such as it is very sensitive to slow blood flow that can disappear such as in veins and small blood vessels. Also, it tends to exaggerate approximately 2.4 to 3.8% due to decreased signals by swirl like it occurs by angiostenosis [14]. Consequently, TOF technique was reported to be sensitive to the flow velocity and form. However, there is no report about the objective evaluation of image changes by blood flow variations. In this study, we tested with actual phantom production how flow variations affect three-dimensional TOF angiography images.

2. Materials and Methods

2.1. Phantom Model

The phantom used in this study was designed to connect with the contrast agent injectors enabling quantitative injection, having a pipe with 2.11 mm in diameter connected with pipes in front and back. In addition, the material of the phantom body was plastic filled with water inside, so it was less affected by X-ray and Radio Frequency. First, a polyethylene tube with 2.11 mm diameter and 0.26 cm^2 area penetrated through plastic cylindrical phantom body. Then inlet and outlet part were connected with tubes to enable the fluid to ship and receive. The phantom body was round with 19 cm in length, 5 cm in height and 5 cm in diameter and was also filled with water (H^2O) as human tissue equivalent material.

2.2. Methods

We used the 3.0T MR System (Achieva Release 2.5, Philips) with an 8Channel SENSE Head Coil (Achieva Release 2.5, Philips) and the image variables were fixed to T1 Fast Field Echo (FFE) 3D TOF and 3D CE MRA in these tests.

3D TOF was examined with 3D fast field echo (FFE) sequence technique with the following parameters: field of view (FOV): 180 × 180 × 12 mm^3, matrix: 400 × 215, TR/TE: 20/3.5 ms, total slice: 25, flip angle: 20°, phase encoding direction R-L, NEX: 1, chunk: 1, slice thickness: 0.5 mm, slice orientation transverse, and total scan time 21.9 sec. 3D CE MRA was using the 3DT1FFE Sequence technique using the following parameters: FOV: 350 × 350 × 80 mm^3, matrix: 716 × 715, TR/TE: 5.4/2.0 ms, total slice: 160, flip angle: 20°, phase encoding direction: R-L, NEX: 1, slice thickness: 0.5 mm, slice orientation: coronal, CE profile: CENTRA, keyhole: no, and total scan time: 61 sec. The fluid for 3D CE MRA was prepared with Ga-DTPA 2.5 ml diluted into 1000 ml of saline solution. The total volume of 150 ml diluted fluid was inserted through the automated injector at 2 ml/sec.

The flow model was non-pulsatile with saline as fluid and it was injected with a flow rate of 0.4 ml/sec by auto injector. Next, the actual flow rate in a conduit was calculated by the following formula.

$$\text{Flow Velocity} = \text{Quantity of Flow/Conduit area} \quad (1)$$

According to the formula, when we injected with 0.4 ml/sec by contrast agent injectors, we could see a flow of 11.4 cm/sec in the tube. The data were obtained as axial, coronal plane images reconstructed by the maximum intensity projection (MIP) method with Xtra Vision workstation (Release 6.2.3). At this time, the reset value provided by the instrument was used as reconfigured histogram setting (Fig. 1).

A first, 1, 5, 10, 15, 20, 25-th cross-section were used for measuring fluid signal strength, phantom body signal strength and background signal intensity were used for measuring signal-to-noise ratio and contrast-to-noise ratio.

Signal to noise ratio was calculated as equation using the

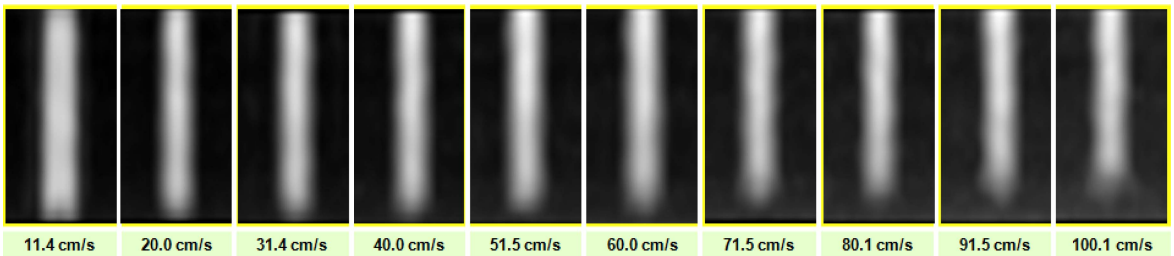

Fig. 1. (Color online) The coronal plane images were acquired using auto injector at a flow rate through 0.4 ml/sec.

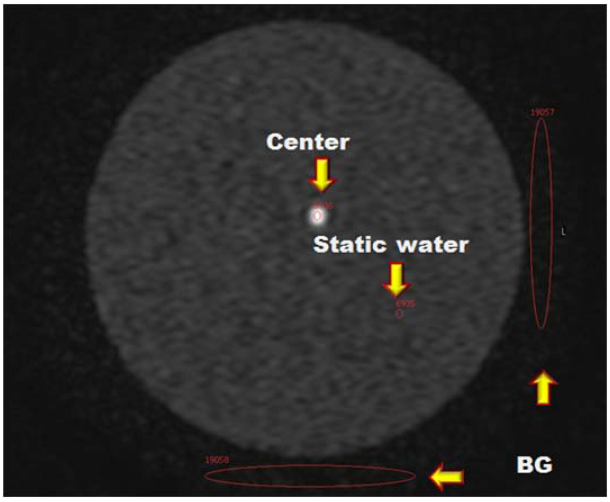

Fig. 2. (Color online) In the axial image was measured the signal strength of fluid, phantom body and background.

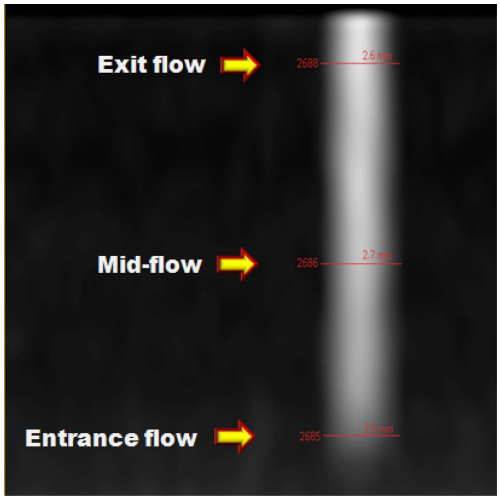

Fig. 3. (Color online) In the coronal image, the length of inlet, middle and outlet part was measured. The measured length was the calculated magnification on the basis of the actual conduit length (2.11 mm).

signal strength of the fluid and phantom body signal intensity divided by the signal strength value of the background standard deviation. Contrast-to-noise ratio was calculated as equation using the difference between the signal strength of the fluid and phantom body signal divided by the signal strength value of the background standard deviation 3. A background standard deviation was shown as the mean value and standard deviation measured in upper left point and lower point of phantom, the phase encoding direction (Fig. 2).

$$\mathrm{SNR} = \frac{\mathrm{SI(region,\ surrounding\ tissues)}}{\mathrm{SDN}} \quad (2)$$

SNR: signal to noise ratio
SDN : standard deviation of noise in the background
SI : signal intensity

$$\mathrm{CNR} = \frac{\mathrm{SI(region)} - \mathrm{SI(surrounding\ tissues)}}{\mathrm{SDN}} \quad (3)$$

CNR: contrast to noise ratio
SDN : standard deviation of noise in the background
SI : signal intensity

In addition, the coronal plane image gained through maximum intensity projection was used for measuring the inlet, intermediate and outlet length. Measured length was calculated on the basis of the actual pipe length (2.11 mm) (Fig. 3). The magnification is calculated as follows.

2.3. Data Processing

The difference measured by fluid velocity between signal-to-noise ratio and contrast-to-noise ratio was used for analysis of variance by ANOVA (ANOVA SPSS win 18.0, USA). The one sample t-test was conducted on the actual measure of 2.11 mm and the measured value that was closest to the actual measurement.

A p-value less than 0.05 was considered as a statistically significant difference. We used IBM's PASW version 18.0 for Windows for the statistical program.

3. Results

3.1. Signal-to-noise ratio and contrast-to-noise ratio measured by fluid velocity

The signal-to-noise ratio by fluid velocity was measured 62.91 ± 12.33 at a fluid speed 11.4 cm/sec; it was 59.40 ± 13.95 at 20 cm/sec and 53.98 ± 14.84 at 31.4 cm/sec. But it was the lowest with 30.28 ± 11.47 at 100.1 cm/sec. As a result, we can find a faster fluid speed reduces the signal-to-noise ratio ($p < 0.05$) (Table 1).

The contrast-to-noise ratio by fluid velocity was measured 55.35 ± 13.93 at 11.4 cm/sec; 51.78 ± 15.53 at 20 cm/sec and was largely measured with 46.63 ± 16.67 at 31.4 cm/sec. It was with 22.48 ± 13.25 the lowest at 100.1 cm/sec. As a result, we can recognize that a faster fluid reduces the contrast-to-noise ratio ($p < 0.05$) (Table 1).

3.2. Cavity length measured by fluid velocity

According to the result of cavity length measured by fluid velocity, the inlet part length was measured 2.60 ± 0.00 mm at 11.4 cm/sec, the middle part length was 2.66 ± 0.05 mm and the outlet part length was 2.63 ± 0.05 mm. The inlet part length was measured 2.60 ± 0.50 mm with a fluid velocity of 100.1 cm/sec, the middle part length was 2.66 ± 0.05 mm and the outlet part length was 2.66 ± 0.05 mm. As a result, there was with 2.66 mm ($p = 0.227$) no difference in the measurement of the cavity length between the inlet, middle and outlet length. The magnification factor

Table 1. Signal-to-noise ratio and contrast-to-noise ratio measured by fluid velocity.

Division	Slice Velocity (cm/sec)	1st Slice	5th Slice	10th Slice	15th Slice	20th Slice	25th Slice	average	P
Signal-to-noise ratio	11.4	41.3	68.3	73.2	68	71.5	55.2	62.91 ± 12.33	0.000
	20	32.2	59.8	63.4	72.4	64.7	63.9	59.40 ± 13.95	
	31.4	24.6	55.4	56.9	65.2	59.2	62.6	53.98 ± 14.84	
	40	20.6	51.5	53.4	54.8	53.9	59.5	48.95 ± 14.14	
	51.5	13.1	40.8	45.6	54.8	53	53.3	43.43 ± 15.81	
	60	12.9	39.2	46.9	51.2	48	54.9	42.18 ± 15.26	
	71.5	11.9	31.1	39.4	47	40.9	47.9	36.36 ± 13.43	
	80.1	12.7	30.9	36.3	38.5	40.4	41.5	33.38 ± 10.08	
	91.5	11.1	24.5	38.6	36.5	40.9	41.6	32.20 ± 12.06	
	100.1	12	20.2	34.4	36.8	37.5	40.8	30.28 ± 11.47	
Contrast-to-noise ratio	11.4	29.8	60.2	65.7	62.3	65.2	48.9	55.35 ± 13.93	0.002
	20	21.4	51.8	56.3	65.5	58.8	56.9	51.78 ± 15.53	
	31.4	13.5	47.7	50.6	58.7	53.8	55.5	46.63 ± 16.67	
	40	9.1	43	45.8	49.3	48.4	53.2	41.46 ± 16.22	
	51.5	3	33	39.1	48.4	47	47.2	36.28 ± 17.36	
	60	0.7	30.6	40	44	42.2	48.6	34.35 ± 17.52	
	71.5	1.1	23.5	33.3	40	35	40.7	28.93 ± 14.97	
	80.1	1	22.2	29.6	32.9	34.3	35.3	25.88 ± 13.07	
	91.5	1.1	16.5	31	30.5	34.5	34.6	24.70 ± 13.35	
	100.1	0.7	11.7	27.5	29.5	31.7	33.8	22.48 ± 13.25	

Table 2. Cavity length measured by fluid velocity.

Slice Velocity (cm/sec)	Entrance-flow			Mid-flow			Exit-flow			P
	Mean (mm)	SD	M.P (%)	Mean (mm)	SD	M.P (%)	Mean (mm)	SD	M.P (%)	
11.4	2.600	0.000	49.000	2.630	0.050	52.300	2.630	0.050	52.300	0227
20.0	2.660	0.050	55.600	2.700	0.000	59.000	2.630	0.050	52.300	
31.4	2.630	0.050	52.300	2.660	0.050	55.600	2.630	0.050	52.300	
40.0	2.700	0.000	59.000	2.700	0.000	59.000	2.600	0.000	49.000	
51.5	2.630	0.050	52.300	2.700	0.000	59.000	2.700	0.000	59.000	
60.0	2.660	0.050	55.600	2.660	0.050	59.000	2.660	0.050	52.300	
71.5	2.630	0.050	55.600	2.630	0.050	55.600	2.600	0.000	55.600	
80.1	2.630	2.600	52.300	2.630	0.050	52.300	2.700	0.000	49.000	
91.5	2.630	0.050	52.300	2.600	0.000	49.000	2.700	0.000	59.000	
100.1	2.660	0.050	55.600	2.660	0.050	55.600	2.660	0.050	55.600	

was from 49 to 55.6% in the inlet part, from 49 to 59% in the middle and from 49 to 59% in the outlet part, meaning that the image is generally larger than the actual size ($p < 0.05$) (Table 2).

3.3. Measurement of lumen length in terms of flow velocity of 3D TOF MRA and 3D CE MRA

From the measurement of lumen length in terms of flow velocity within the conduit, the smallest measure was 2.51 ± 0.12 mm with a velocity of 40.0 cm/sec. For 3D TOF MRA, the value measured at 40 cm/sec, which was the closest value to the actual measurement, was 0.40 mm larger than the actual measure. 3D CE MRA conducted using 3.0 Tesla examination produced a value 0.50 mm larger than the actual value (Table 3).

Table 3. Measurement of lumen length in terms of flow velocity of 3D TOF MRA and 3D CE MRA.

Equipment	(Mean - 2.11) mm	P
3D TOF MRA (velocity : 40 cm/s)	0.40	0.00
3D CE MRA	0.50	0.00

4. Discussion

MRI has been established as the primary diagnostic tool of brain nervous diseases with superior soft tissue contrast than any other road tests. Cross-sectional images, anatomical and functional images as well as an assessment of the metabolites are possible without radiation. So it can be called the most advanced testing method. In the early days of clinical application, the diagnostic rate of vascular obstruction diseases was not very high, but more than 85% sensitivity and close to 100% specificity were shown according to an increasingly advanced fast-resolution recording technology in recent years [8, 9, 15]. In addition, MRA also has been rapidly developed with the development of MRI. MRA is with morphological and hemodynamic information of blood vessels one field of MRI. Dual TOF MRA technique mainly provides information of vascular morphology and has been widely used because of its relatively short duration time and high resolution images of blood vessels [16, 17]. The principle of the TOF MRA minimize the strength of the signal from suspended substances and maximize the signal strength of flow rate, so it can maximize the contrast between two quantum [18]. Clinically, the strength of flow rate at TOF MRA is greatly influenced by many variables that are divided into the variables related to imaging techniques and the nature of the fluid. First, variables related to imaging techniques are repetition time, echo time, flip angle and slice thickness [18]. Next, variables related to the fluid nature include fluid velocity, flow properties and form of the flow [18]. In particular, the reducing effect on the signal is generated according to the speed and form of the flow. Clinically, reflux and swirling within a blood vessel cause signal reduction in magnetic resonance vessel test, so it shows a different image from the actual picture [19-22]. In order to represent the correct blood vessel pattern, we minimized the influence from the decreasing signal using the MIP techniques [21]. Consequently, TOF technique was reported as sensitive to flow velocity and form. However, the objective evaluation of image change according to the change of blood flow rate is not reported. In this study, we evaluated how the flow phenomena affect the TOF images in a three-dimensional TOF MRA with producing a real phantom. The phantom is made of a pipe ofpolyethylene plastic material and saline was used as the fluid. Blood is a non newton liquid with viscosity. There are a number of factors such as red blood cells and other particles and a pulse as well as elasticity and resistance of the blood vessels [23, 24]. However, the present study was conducted with some of the factors only because it is difficult to quantify all factors.

In this study, the signal-to-noise ratio by fluid velocity was measured 62.91 ± 12.33 at the speed of 11.4 cm/sec. It was the lowest with 30.28 ± 11.47 at 100.1 cm/sec. The contrast-to-noise ratio by the fluid velocity was measured 55.35 ± 13.93 at 11.4 cm/sec. It was the lowest with 22.48 ± 13.25 at 100.1 cm/sec. As a result, we know that a faster fluid decreases the signal-to-noise ratio and the contrast-to-noise ratio. Choi *et al.* [25] conducted their study with the result that variations of the flow rate, signal-to-noise ratio and contrast-to-noise ratio are increasing according to a decreasing fluid velocity. The same results were obtained in our study. It is theoretically reported the signal strength of the fluid speed increases in proportion to the fluid velocity until it reaches the threshold. However, in the present study, the faster fluid velocity, the lower fluids signal intensity. Choi *et al.* [25] reported it should be considered as phase effect in addition to the TOF effect., The phase change of spin by motion is represented by φ in the gradient echo technique, so the speed increases in proportion to velocity if the other variables are constant [25, 26]. In this study, the flow rate was increased, a laminar flow was formed and the speed difference between the center and periphery in the laminar flow led to an increase in the phase differences because we used saline with a lower viscosity than blood. Therefore, it is thought that the signal strength of the fluid was decreased due to the dispersion effect of phase. We used one-dimensional flow-compensation-gradient magnetic field to constantly eliminate the phase differences caused by the fluid flowing. However, the phase differences by various velocities were not overcome, so the signal strength was decreased in this case [25, 27]. As a result, the fluid velocity increasesand it is considered that the phase dispersion effect acts larger than the effect TOF.

As the result of length of inner cavity by fluid velocity, the length of inlet, middle and outlet part were measured with each 2.66 mm with no differences, the magnification of measured length was enlarged than actual measurement, the inlet part was from 49 to 55.6%, the middle part was 49 to 59% and the outlet part was 49%-59%, respectively. Choi *et al.* [25] measured the signal intensity of inlet and outlet part by the contrast media. In that study, even though the concentration of contrast agent was high, the signal intensity changes in the inlet and outlet parts were insignificant. In this study, not the signal strength, but the length of the actual inlet, middle, outlet part was measured. As a result, there were no changes observed in the lengths of the inlet part and the outlet part. The images showed larger than actual measurement in the magnification factor. The image may be enlarged because we used the MIP method as image reconstruction technique. Clinically, MIP images from MRA data are used to analyze the presence or absence of abnormal kinds of cerebral artery disorders such as cerebral aneurysm. MIP images are widely used because of its high implementation rate in blood vessels [28, 29]. However, there is a disadvantage that the spatial distribution of the blood vessel is unknown because due to the three-dimensional cerebrovascular data projected to two-dimensional surface occurred a depth loss of information in

the normal maximum intensity projection image. In addition, when more than two vessels overlap at the direction, it is difficult to determine abnormalities in vessels [30, 31]. Also, the image is expanded by changing the pixels during the course of post data processing [30, 31]. So, the enlarged images were come from image size changes by reconstitution.

As a limitation of this study there are a number of differences with the real blood circulation within a human body human because a simplified model was used for the present study. First, the fluid viscosity is lower than blood and T1 value shows big. T1 value is typically affected by external conditions such as the temperature of surrounding tissues and viscosity of the material. As concentration of the substance increases, the video signal strength is linearly proportional and of high strength. Therefore, it is difficult to measure the correct signal strength comparing the fluid material used in this study and blood flow. Second, the blood circulation is a pulsatory flow caused by heartbeat, but in this study we used a continuous flow with a constant velocity. Third, fluid flow passage is different from the actual vascular structure. Therefore, such differences should be considered if those results were utilized in the clinical service.

5. Conclusion

Consequently, 3D TOF MRA shows that the signal-to-noise ratio and the contrast-to-noise ratio is decreasing with a faster fluid and is determined that a larger image was displayed through this study. The characterization of the fluid signal strength using the experimental model is helpful to understand the principle of MRA, also it can be used as base material to design an experimental model.

Acknowledgments

Eng-Chan Kim, Yeong-Cheol and Jae-Hwan Cho equally contributed to this work. They are co-first authors. This work was supported by the Soonchunhyang University Research Fund (No. 20130580).

References

[1] H. J. Lee, O. K. Park, J. C. Kang, Y. K. Shin, S. L. Lee, and M. S. Jung. J. Korean. Med. Assoc. **34**, 758 (1991).
[2] H. J. Myung, S. B. Lee, J. K. Rho, B. W. Y, W. Y. Lee, M. H. Kim, J. H. Kim, B. A. Wie, C. S. Chung, and O. S. Kwon, Korean J. Neurology **7**, 179 (1989).
[3] I. H. Song, D. H. Oh, H. S. Kang, C. H. Cho, K. S. Kim, M. S. Kim, J. S. Song, and J. H. Bae, Korean J. Med. **43**, 637 (1992).
[4] B. C. Lee, S. C. Jeong, S. H. Hwang, H. C. Kim, J. C. Bae, H. I. Ma, K. H. Yu, and I. H. Lee, Korean J. Stroke **1**, 21 (1999).
[5] P. Schramm, P. D. Schellinger, E. Klotz, K. Kallenberg, J. B. Fiebach, S. Külkens, S. Heiland, M. Knauth, and K. Sartor, Stroke **35**, 1652 (2004).
[6] S. K. Lee, Korean J. Stroke **10**, 89 (2008).
[7] C. G. Choi, D. H. Lee, J. H. Lee, H. W. Pyun, D. W. Kang, S. U. Kwon, J. K. Kim, S. J. Kim, and D. C. Suh, AJNR Am. J. Neuroradiol **28**, 439 (2007).
[8] J. E. Heiserman, B. P. Drayer, E. K. Fram, P. J. Keller, C. R. Bird, J. A. Hodak, and R. A. Flom, Radiology **182**, 761 (1992).
[9] J. E. Heiserman, B. P. Drayer, P. J. Keller, and E. K. Fram, Radiology **185**, 667 (1992).
[10] Y. Korogi, M. Takahashi, T. Nakagawa, N. Mabuchi, T. Watabe, Y. Shiokawa, H. Shiga, T. O'Uchi, H. Miki, Y. Horikawa, S. Fujiwara, and M. Furuse, AJNR Am. J. Neuroradiol **18**, 135 (1997).
[11] A. H. Wilman, S. J. Riederer, B. F. King, J. P. Debbins, P. J. Rossman, and R. L. Ehman, Radiology **205**, 137 (1997).
[12] F. R. Korosec, R. Frayne, T. M. Grist, and C. A. Mistretta, Magn. Reson. Med. **36**, 345 (1996).
[13] V. L. Yarnykh, M. Terashima, C. E. Hayes, A. Shimakawa, N. Takaya, P. K. Nguyen, J. H. Brittain, M. V. McConnell, and C. Yuan, J. Magn. Reson. Imaging **23**, 691 (2006).
[14] J. M. U-King-Im, R. A. Trivedi, M. J. Graves, N. J. Higgins, J. J. Cross, B. D. Tom, W. Hollingworth, H. Eales, E. A. Warburton, P. J. Kirkpatrick, N. M. Antoun, and J. H. Gillard, Neurology **62**, 1282 (2004).
[15] Q. Wu and M. H. Li, BMC Neurology **12**, 1471 (2012).
[16] P. M. Ruggieri, G. A. Laub, T. J. Masaryk, and M. T. Modic, Intracranial circulation: pulse-sequence considerations in three-dimensional (volume) MR angiography. Radiology **171**, 785 (1989).
[17] J. S. Lewin and G. Laub, Intracranial MR angiography: a direct comparison of three time-of-flight techniques. AJNR Am. J. Neuroradiol. **12**, 1133 (1991).
[18] C. Altin, JAVA applets for simulation of magnetic resonance imaging. The graduate school of natural and applied sciences, middle easttechnical university, 2008.
[19] T. S. Jung, Y. C. Lim, S. H. Seo, K. H. Kim, and E. H. Kim, J. Korean Radiol. Soc. **33**, 189 (1995).
[20] R. R. Edelman, H. P. Mattle, B. Wallner, R. Bajakian, J. Kleefield, C. Kent, J. J. Skillman, J. B. Mendel, and D. J. Atkinson, Radiology **177**, 45 (1990).
[21] C. M. Anderson, D. Saloner, J. S. Tsuruda, L. G. Shapeero and R. E. Lee, AJR Am. J. Roentgenol. **154**, 623 (1990).
[22] A. M. Masaryk, J. S. Ross, M. C. DiCello, M. T. Modic, L. Paranandi, and T. J. Masaryk, Radiology **178**, 797 (1991).
[23] K. Perktold, T. Kenner, D. Hilbert, B. Spork, and H. Florian, Basic. Res. Cardiol. **83**, 24 (1988).
[24] K. Perktold, J. Biomech. **20**, 311 (1987).
[25] C. K. Choi, M. H. Han, J. H. Park, and K. H. Jang, J. Korean Radiol. Soc. **36**, 729 (1997).

[26] R. J. Alfidi, T. J. Masaryk, E. M. Haacke, G. W. Lenz, J. S. Ross, M. T. Modic, A. D. Nelson, J. P. LiPuma, and A. M. Cohen, AJR Am. J. Roentgenol. **149**, 1097 (1987).
[27] G. W. Lenz, E. M. Haacke, T. J. Masaryk, and G. Laub, Radiology **166**, 875 (1988).
[28] C. Jackowski, E. Aghayev, M. Sonnenschein, R. Dirnhofer, and M. J. Thali, International Journal of Legal Medicine **120**, 165 (2006).
[29] S. H. Shin and D. S. Hwang, JKSMRM **16**, 67 (2012).
[30] E. K. Fishman, D. R. Ney, D. G. Heath, F. M. Corl, K. M. Horton, and P. T. Johnson, Radiographics **26**, 905 (2006).
[31] J. Lee, T. S. Chung, K. Y. Lee, and S. H. Suh, J. Korean Soc. Magn. Reson. Med. **15**, 234 (2011).